Full correction of the self-absorption in soft-fluorescence extended x-ray-absorption fine structure

L. Tröger, D. Arvanitis, and K. Baberschke
Institut für Experimentalphysik, Freie Universität Berlin, Arnimallee 14, D-1000 Berlin 33, Federal Republic of Germany

H. Michaelis, U. Grimm, and E. Zschech
Institut für Keramische Werkstoffe, Bergakademie Freiberg, Gustav-Zeuner-Strasse 3, D-9200 Freiberg, Federal Republic of Germany

(Received 22 January 1992)

The amplitude of the extended x-ray-absorption fine structure of concentrated samples measured in the fluorescence mode (FLEXAFS) as well as the overall shape of the fluorescence-yield spectra strongly depend on the detection geometry through the self-absorption effect. In these cases, a conventional EXAFS analysis can lead to systematic errors in the determination of physical parameters. We studied the distortions in the FLEXAFS spectra through the self-absorption effect measuring the FLEXAFS of a NiO single crystal above the oxygen K edge for various detection geometries. We show that knowing the stoichiometry of the sample we can *fully* correct for the self-absorption effect using a simple theory and obtain the correct, geometry-independent oxygen EXAFS of NiO. The correction procedure presented here for the prototype system of NiO is generally applicable and should be the first step in the analysis of FLEXAFS data of concentrated samples. We calculate the information depth of the fluorescence detection as a function of the experimental geometry. The knowledge of the self-absorption in relationship to the information depth allows the determination of the optimum experimental setup.

I. INTRODUCTION

Extended x-ray-absorption fine structure (EXAFS) spectroscopy is increasingly used in order to determine the local atomic environment around a particular atomic species of a sample. Most commonly, the x-ray absorption of bulk samples is measured in a transmission experiment. However, particularly in the soft x-ray region this method is usually not applicable since it would require the preparation of extremely thin (~ 1000 Å) and homogeneous films. Therefore, EXAFS and surface EXAFS of light elements like oxygen were generally measured in a reflexion geometry by electron yield (EY) detection since the fluorescence yield (FY) decreases with decreasing atomic number and Auger transitions are the dominant deexcitation channels of the $1s$ core hole.[1] For higher x-ray energies (heavier atoms) the FY detection of EXAFS has been used alternatively to the transmission method since its development by Jaklevic *et al.*[2] The development of high-performance fluorescence detectors[3–6] within the past few years established this method in the soft x-ray region as well.

FY detection has a number of advantages with respect to the other methods. It is, for instance, applicable to insulating materials and it has a higher signal-to-background ratio in comparison to the EY detection[4] and the transmission method. Furthermore, the information depth in FY detection is typically much larger than in EY detection making this technique a useful tool to investigate the bulk properties of the sample.[7] In the limit of thin films or dilute samples (samples where the absorption due to the central atom is much smaller compared to the absorption of the other atoms within the sample) the FY intensity is directly proportional to the central atom absorption coefficient of interest[2] and therefore the extraction of the EXAFS is straightforward. In the case of concentrated (and thick) samples, however, a systematic, energy dependent reduction in the experimentally measured fluorescence EXAFS (FLEXAFS) amplitude called self-absorption (or reabsorption) occurs in a reflexion setup. This reduction depends on the attenuation experienced by the penetrating (incident) and escaping (fluorescence) x-ray radiation while propagating through the sample.[8] In these cases, a conventional EXAFS analysis can lead to errors in the determination of physical parameters related to the EXAFS amplitude in excess of 50%. Recently, Tan *et al.*[9] discussed differences in coordination numbers and Debye-Waller factors determined from the experimentally measured FLEXAFS spectra (in the following called "experimental EXAFS") of transition metals and from the physically true EXAFS (in the following called "true EXAFS"). For a special experimental fluorescence detection setup under a small angle with respect to the sample surface the distortions of the experimental EXAFS are negligible.[10,11] In a recent study of the high-temperature superconductor $YBa_2Cu_3O_7$ it has been shown that a correction of the self-absorption effect is necessary for a quantitative understanding of the angular dependence of the FY spectra.[12] In this paper we study systematically the self-absorption effect above the oxygen K edge of a NiO single crystal. Depending strongly on the detection geometry, the experimental EXAFS amplitude varies up to 45% as a function of x-ray incidence angle as has been also shown recently.[13] However, for a cubic symmetry crystal like NiO the true EXAFS is independent of the detection geometry.

We show that based on an expression for the experimental EXAFS given by Goulon *et al.*[14] we can fully correct amplitude distortions due to the self-absorption effect. A discussion for the amplitude correction due to an incomplete background removal is included. Most important, the correction of the self-absorption effect is made directly in k space previous to all further data analysis procedures. It does not assume any particular energy dependence of the self-absorption, as in Ref. 9, and can, under certain experimental conditions given in Sec. IV, be applied whenever the stoichiometry of the sample is known. The paper is structured as follows. The experimental setup is described in Sec. II. In Sec. III, the theory of the FY intensity is given and compared with the experimental results. Section IV shows how to correct the self-absorption effect in FLEXAFS spectra and Sec. V discusses the information depth of the FY detection.

II. EXPERIMENT

The experiments were performed at the storage ring BESSY using the plane-grating grazing-incidence monochromator HE-PGM2 which covers the soft x-ray energy range up to 2 keV.[15] A flux of about 10^9 photons/s with an energy resolution of ~ 2 eV was obtained at the O K edge (533 eV). The experimental setup was similar to earlier studies[4,7] (see Fig. 1). A NiO(100) wafer of 12-mm diameter and 1-mm thickness as well as a polycrystalline graphite sample (for normalization) were mounted in an ultrahigh vacuum chamber. The sample holder was rotatable to vary the x-ray incidence angle ϕ with respect to the sample surface. The flux of the monochromatized synchrotron radiation was monitored by measuring the photocurrent from a high transmission gold grid. The x-ray fluorescence radiation was detected with a windowless Si(Li) detector[3,5] positioned along the electric field vector (Fig. 1). Total electron yield (TEY) spectra were measured with a channeltron. For x-ray energies higher than about 860 eV, the two main contributions of the NiO fluorescence signal could clearly be resolved: the O $K\alpha$ fluorescence at ≈ 525 eV and the Ni $L\alpha$ fluorescence at ≈ 852 eV. The oxygen FY spectra were recorded with an electronic window positioned around the O $K\alpha$ peak isolating only the oxygen fluorescence radiation.

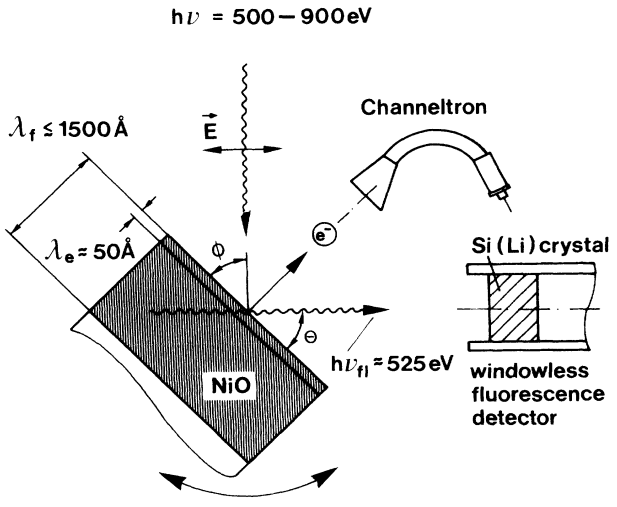

FIG. 1. The experimental setup showing schematically the FY and TEY detection. The fluorescence detection geometry is characterized by the angles ϕ and θ of the incident and detected fluorescence photon direction with respect to the sample surface, respectively. The information depth of the FLEXAFS method depends strongly on the detection geometry, see Fig. 5.

FLEXAFS spectra of the NiO crystal were taken for six different angles of x-ray incidence $\phi = 10°, 25°, 40°, 55°, 70°, 85°$ (see Fig. 1, $\theta = 90° - \phi$) at liquid nitrogen temperature. The energy of the incident x-rays was scanned between 500 and 900 eV with a step width of 2 eV, covering the oxygen EXAFS range up to the Ni L edges. The fluorescence detector worked linearly up to a maximal count rate of about 15 000 counts/s. To achieve a good signal-to-noise ratio of the FY spectra, about 10 scans of ~ 10 min each were accumulated. The FY raw spectra were normalized for the photon flux by dividing with the photocurrent obtained from the gold grid. However, also the TEY and FY spectra of the graphite sample yielded smooth functions proportional to the monochromator's transmission function and could be used for normalization. By comparison of the experimental EXAFS spectra and their Fourier transforms we checked that the different possibilities of normalization gave the same result within the experimental noise. Figure 2 shows normalized FY spectra of the NiO crystal at liquid nitrogen temperature for a (a) grazing and (b) normal x-ray incidence angle ($\phi = 10°$ and 85°, respectively). Note the high edge-jump ratio (defined as: the size of the edge jump divided by the background yield) of around 35 at the oxygen K edge. The dashed lines are the splines used for the determination of the experimental EXAFS.

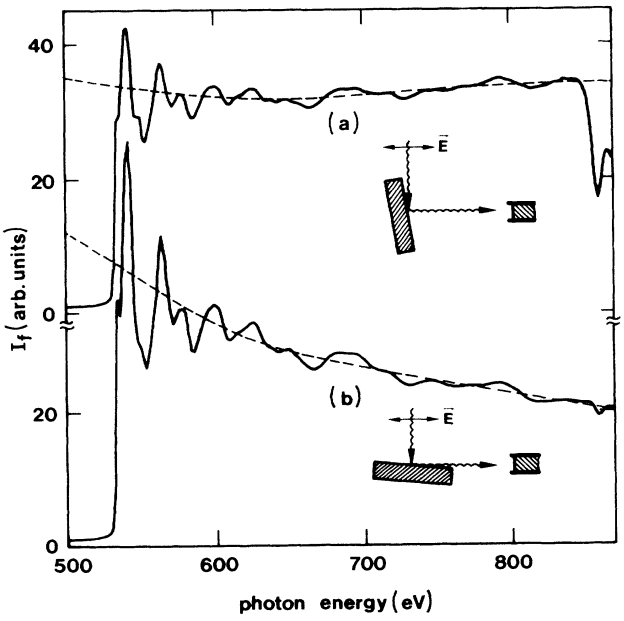

FIG. 2. Normalized FY spectra of a NiO single crystal at liquid nitrogen temperature for (a) grazing ($\phi = 10°$) and (b) normal ($\phi = 85°$) x-ray incidence. The dashed lines are the splines used to obtain the experimental EXAFS spectra.

III. THEORY OF THE FLUORESCENCE YIELD INTENSITY

Summing all oxygen $K\alpha$ fluorescence photons generated along the penetration path of the incident x-rays within the sample that reach the fluorescence detector we obtain the total measured oxygen $K\alpha$ FY intensity, I. The contribution to I, $dI(y)$, originating from the atoms located in the depth y to $y+dy$ along the penetration path of the incident photon beam is proportional to (i) the incident photon flux I_0, (ii) the absorption coefficient μ_0 due to the core-hole creation process of the oxygen K shell, (iii) the fluorescence yield ϵ_O of the oxygen K shell, and (iv) the solid angle covered by the fluorescence detector and is given by

$$dI(E,y) \propto \frac{A}{r^2} I_0(E)\epsilon_O \mu_O(E) \exp[-\mu_{tot}(E)y - \mu_{tot}(E_f)z]dy, \quad (1)$$

where the variable z measures the path length of the escaping fluorescence photons. In Eq. (1), A denotes the active area of the FY detector at a distance $r \gg \sqrt{A}$ from the sample. The two exponential terms in Eq. (1) arise from the fact that the incident photon beam of energy E as well as the detected oxygen $K\alpha$ fluorescence radiation of energy $E_f = 525$ eV are attenuated while traveling the distance y and z through the sample, respectively. μ_{tot} is the total absorption coefficient (due to the oxygen and all other elements) of the sample. The detected oxygen $K\alpha$ FY intensity is the sum of all contributions of Eq. (1). We assume a plane sample surface and the detection geometry of Fig. 1, i.e., an angle ϕ of the incident x rays and an angle θ of the detected fluorescence radiation with respect to the sample surface. Introducing the depth variable $x = y\sin\phi = z\sin\theta$ giving the depth perpendicular to the sample surface, the normalized oxygen $K\alpha$ FY intensity of a sample of thickness d as a function of the incident photon energy E is then given by

$$I/I_0(E) \propto \frac{A}{r^2}\epsilon_O \mu_O(E) \frac{1}{\sin\phi} \int_0^d \exp\left[-\left[\frac{\mu_{tot}(E)}{\sin\phi} + \frac{\mu_{tot}(E_f)}{\sin\theta}\right]x\right]dx$$

which yields[2,14]

$$I/I_0(E) \propto \frac{A}{r^2}\epsilon_O \frac{\mu_O(E)}{\mu_{tot}(E)+\mu_{tot}(E_f)\frac{\sin\phi}{\sin\theta}} \left[1-\exp\left[-\left[\frac{\mu_{tot}(E)}{\sin\phi} + \frac{\mu_{tot}(E_f)}{\sin\theta}\right]d\right]\right]. \quad (2)$$

For a more detailed discussion of Eq. (2) and its limitations see Ref. 16. In the case of thick samples with respect to the penetration depth of the photons, i.e.,

$$\left[\frac{\mu_{tot}(E)}{\sin\phi} + \frac{\mu_{tot}(E_f)}{\sin\theta}\right]d \gg 1,$$

no incident x rays are penetrating through the bulk and the exponential term can be neglected. The normalized oxygen fluorescence intensity I_f obtained from the experiment is then given after Eq. (2) by

$$I_f(E) \propto \frac{A}{r^2}\epsilon_O \frac{\mu_O(E)}{\mu_{tot}(E)+\mu_{tot}(E_f)g} f(E) + I_{bac}(E) \quad (3)$$

with the factor $g = \sin\phi/\sin\theta$ characterizing the experimental detection geometry, $I_{bac}(E)$ the background function, and $f(E)$ a smooth function due to the normalization. In our setup, it is $\theta = 90° - \phi$ and therefore $g = \tan\phi$. The background function seen in Fig. 2 below the oxygen K edge contains mainly second-order O $K\alpha$ contributions. As expected, the FY intensity of Eq. (3) depends on the absorption coefficient of the oxygen K shell. However, the additional dependence on the total absorption coefficient at both the incident and fluorescence photon energies causes the self-absorption and determines the shape of the spectra. Through the geometrical factor g both are dependent on the detection geometry. For dilute samples, the self-absorption effect is negligible although the shape of the FY spectra still depends on the detection geometry. In the following, we demonstrate the consequences of Eq. (3) in the case of the *concentrated* NiO sample, where $\mu_O \gtrsim \mu_{tot} - \mu_O$. In the normalized FY spectra of Figs. 2(a) and 2(b), the factor g takes the values of $g = 0.176$ for grazing ($\phi = 10°$) and $g = 11.43$ for normal x-ray incidence ($\phi = 85°$), respectively. Not only changes in the overall shape of the spectra are observed but also a reduction of the EXAFS wiggle amplitudes in the 10° spectrum (normalized to the energy-dependent edge jump) with respect to the 85° spectrum. We discuss the former first.

As the incident photon energy is increased from little above the oxygen K edge to higher energies, both the absorption coefficient μ_O of the oxygen K shell and, proportionally, the density of the photoexcited oxygen atoms near the sample surface decrease. As a consequence, the FY intensity of the $\phi = 85°$ spectrum in Fig. 2(b) should decrease proportionally to μ_O as well, since only fluorescence photons generated near the sample surface can reach the fluorescence detector. In the $\phi = 10°$ geometry, however, even the fluorescence photons originating from regions of the sample where the incident photon flux is already considerably attenuated have to travel only a small distance to the surface of the sample and therefore reach the fluorescence detector. For a concentrated sample, the *total* number of photoexcited oxygen atoms for a normalized incident photon flux, proportional to

$\mu_O(E)/\mu_{tot}(E)$, decreases less than μ_O itself. The FY intensity of the 10° spectrum should therefore decrease less than the 85° spectrum. This is seen in Fig. 2. The sharp decrease of the O $K\alpha$ FY intensity at the Ni L_{III} edge around 860 eV in Fig. 2 is due to the additional Ni L absorption which reduces the total number of photoexcited oxygen atoms within the sample. Therefore, in the 10° x-ray incidence spectrum a reduction of the O $K\alpha$ FY intensity is measured. However, the density of the photoexcited oxygen atoms near the sample surface is *unchanged by the additional Ni L absorption.* Only a small effect of the Ni L edge on the 85° spectrum is therefore seen. Equation (3) describes the above considerations quantitatively, with a geometrical factor $g=11.43$ for the 85° spectrum and $g=0.176$ for the 10° spectrum.

IV. CORRECTION OF THE SELF-ABSORPTION EFFECT

The self-absorption effect in the FY intensity, i.e., the damping of oscillations in $\mu_O(E)$, is also seen from Eq. (3). $\mu_{tot}(E)$ contains $\mu_O(E)$, damping the oscillations of $\mu_O(E)$ in the nominator. The self-absorption effect is the stronger the more concentrated the fluorescing (oxygen) atoms are within the bulk sample, the smaller the geometrical factor g is, and the smaller the absorption of the fluorescing photons in the sample is [see denominator in Eq. (3)]. Following similar arguments as for the explanation of the shape of the FY spectra, self-absorption is small for large g's (85° spectrum), since near the sample surface the density of photoexcited oxygen atoms is proportional to μ_O and only O $K\alpha$ photons originating there can reach the fluorescence detector. On the contrary, self-absorption is larger for small g's (10° spectrum) since O $K\alpha$ photons from all along the penetration path of the incident x-rays can reach the fluorescence detector and the total number of photoexcited oxygen atoms shows for a concentrated sample less variation than μ_O itself. In the following, the self-absorption is calculated quantitatively.

The true oxygen EXAFS is defined as

$$\chi_O=\frac{\mu_O(E)-\bar{\mu}_O(E)}{\bar{\mu}_O(E)}\ , \tag{4}$$

where $\bar{\mu}_O$ is the atomic absorption coefficient of the oxygen K shell. With $\mu_{tot}=\mu_O+\mu_{bac}$ (μ_{bac} is the absorption coefficient of all other shells except the oxygen K shell) and assuming a smooth μ_{bac} one can also write

$$\chi_O=\frac{\mu_{tot}(E)-\bar{\mu}_{tot}(E)}{\bar{\mu}_{tot}(E)-\mu_{bac}(E)}\ . \tag{5}$$

In analogy to this expression we are determining the experimental EXAFS from the FY intensity as

$$\chi_{expt}=\frac{I_f(E)-\bar{I}_f(E)}{\bar{I}_f(E)-I_{bac}(E_0)}\ , \tag{6}$$

assuming a constant background $I_{bac}(E_0)$. The experimental EXAFS χ_{expt} differs from the true EXAFS χ_O. Assuming a smooth absorption coefficient of all the other atoms within the sample except the central absorbing atom (oxygen), i.e., no absorption edges, and having a smooth background function, one gets from Eqs. (3)–(6) the relationship

$$\chi_{expt}=\chi_O\left[1-\frac{\mu_O(E)}{\mu_{tot}(E)+\mu_{tot}(E_f)g}\right]\left[\frac{1}{1+\dfrac{\Delta I_{bac}(E)}{cf(E)}\dfrac{\bar{\mu}_{tot}(E)+\bar{\mu}_{tot}(E_f)g}{\bar{\mu}_O(E)}}\right]$$

$$\approx\chi_O\left[1-\frac{\bar{\mu}_O(E)}{\bar{\mu}_{tot}(E)+\bar{\mu}_{tot}(E_f)g}-\frac{\Delta I_{bac}(E)}{cf(E)}\frac{\bar{\mu}_{tot}(E)+\bar{\mu}_{tot}(E_f)g}{\bar{\mu}_O(E)}\right]\equiv\chi_O[1-S(E)-B(E)]$$

$$\text{with } \Delta I_{bac}(E)=I_{bac}(E)-I_{bac}(E_0) \text{ and } c=A/r^2\epsilon_O\ . \tag{7}$$

The second term in large parentheses of Eq. (7), which we call S, describes the reduction of the experimental EXAFS amplitude through the self-absorption effect and was first given by Goulon *et al.*,[14] the third term which we call B, is due to the effect of an uncertain background subtraction on the experimental EXAFS.[16] Higher-order corrections, given also in Ref. 14, are neglected. As seen from Eq. (7), the self-absorption does not affect the EXAFS phases but only the EXAFS amplitudes. As a consequence of Eq. (7), the Fourier transform of the experimental EXAFS is the convolution of the Fourier transform of the true EXAFS and the Fourier transform of $(1-S-B)$.

Figure 3(a) shows the experimental EXAFS of NiO at liquid nitrogen temperature for the two detection geometries with $g=11.43$ (dashed line) and $g=0.176$ (solid line), corresponding to the FY spectra of Fig. 2(a), $\phi=85°$, and Fig. 2(b), $\phi=10°$, respectively. The strong damping of the experimental EXAFS amplitude according to the self-absorption effect for the grazing x-ray incidence angle of $\phi=10°$ with respect to the normal incidence data is seen. The absorption coefficients occurring in the self-absorption term S of Eq. (7) can be calculated from the atomic subshell photoionization cross sections[17] and the stoichiometry of the sample.[18] We used $\rho_{Ni}(NiO)=5.24$ g/cm^3 and $\rho_O(NiO)=1.43$ g/cm^3 given from the experimental density of NiO $\rho=6.67$ g/cm^3.[19] Figure 4 shows the calculated self-absorption term S for

the detection geometries corresponding to $\phi = 10°$, 25°, 40°, 55°, 70°, 85°, 88° (and $\theta = 90° - \phi$) as a function of the photoelectron wave vector $k = \sqrt{2m/\hbar^2(E - E_0)}$ with $E_0 = 533$ eV being the energy of the oxygen K edge. As expected, the smaller the angle ϕ of the incident photons with respect to the sample surface, the larger the self-absorption is. Only for $\phi \gtrsim 88°$ it is less than 3% and therefore negligible, corresponding to an exit angle of the fluorescence photons from the sample surface of $\lesssim 2°$. This is consistent with the findings of Pease *et al.* for FY of copper.[11] In a first-order approximation of Eq. (7) neglecting the term B and taking the results of Fig. 4, the experimental EXAFS χ_{expt} can be corrected for the self-absorption effect by calculating $\chi_{expt}(1-S)^{-1}$ which should give the true EXAFS χ_O. For a cubic crystal, like NiO, χ_O is independent of the detection geometry.

Figure 3(b) shows the experimental EXAFS spectra of Fig. 3(a) ($\phi = 10°$, solid line, and $\phi = 85°$, dashed line) after having applied this simple correction. Almost identical EXAFS spectra within the noise are achieved which demonstrates that the self-absorption effect can be *fully corrected*. For the sake of clarity we have shown in Fig. 3

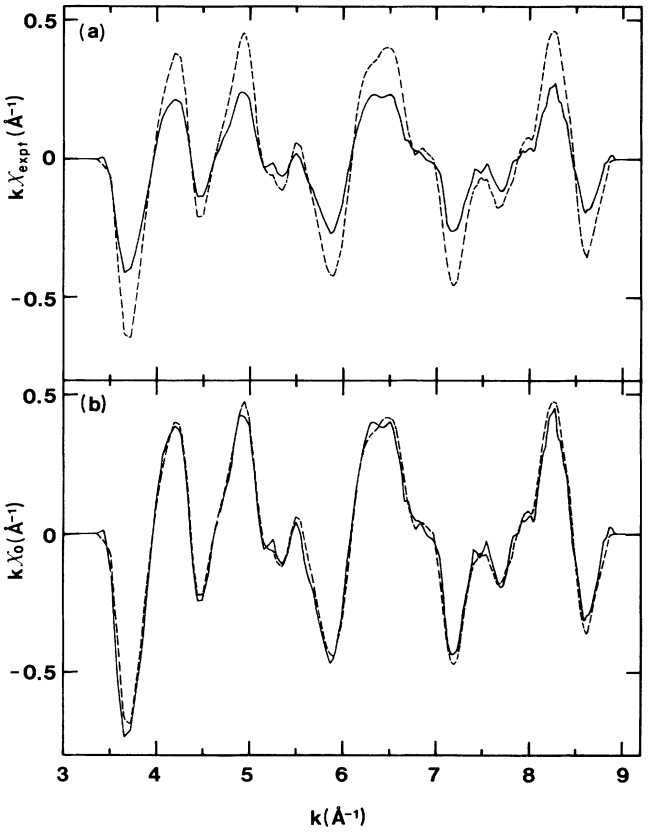

FIG. 3. (a) The experimental FLEXAFS $k\chi_{expt}(k)$ of NiO determined from Fig. 2 for grazing ($\phi = 10°$, $g = 0.176$, solid line) and normal ($\phi = 85°$, $g = 11.43$, dashed line) x-ray incidence. The strong damping of the EXAFS amplitude seen for $\phi = 10°$ is due to the self-absorption effect. (b) The spectra from (a) after the correction of the self-absorption effect (see text). Almost identical spectra are obtained corresponding to the physically true EXAFS $k\chi_O(k)$ of NiO.

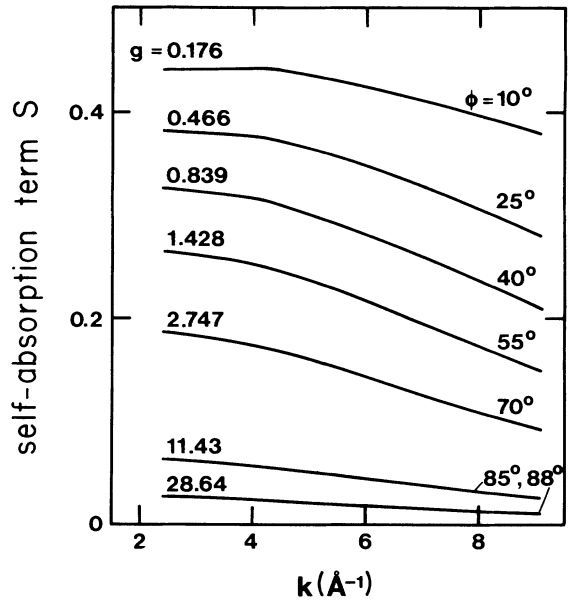

FIG. 4. The self-absorption term $S = \bar{\mu}_O(E)/[\bar{\mu}_{tot}(E) + \bar{\mu}_{tot}(E_f)g]$ for NiO for different detection geometries as a function of photoelectron wave vector k. Only for $88° \lesssim \phi < 90°$, S is smaller than 3% and therefore negligible. For the conversion to k values the energy of the oxygen K edge $E_0 = 533$ eV was used.

only the EXAFS spectra for the most different detection geometries but the correction works for all detection geometries yielding the true EXAFS spectrum. It is important that the correction is made directly in k space previous to all data-analysis procedures. After having applied this correction, the conventional EXAFS analysis can be performed without any changes. The very small deviations between the two corrected spectra in Fig. 3(b) are due to the unknown background function yielding a nonzero term B in Eq. (7) [$\Delta I_{bac}(E) \neq 0$] or due to errors in the determination of ϕ and θ which are affecting the geometrical factor g. The effect of the background removal on the experimental EXAFS amplitude scales with the (energy-dependent) oxygen edge-jump ratio. But even in our case with high edge-jump ratios of $\approx 20-40$ the error on the experimental EXAFS amplitude may be 5–10%. It seems that the accuracy with which physical parameters associated with the EXAFS amplitude can be determined from the self-absorption corrected spectra is not limited through the quality of our correction.

We summarize below the four main conditions which have to be fulfilled in order to be able to apply the correction of the self-absorption effect in the form given above.

(1) The stoichiometry of the sample needs to be known.

(2) The sample is thick with respect to the penetration depth of the incident x rays.

(3) The sample surface is plane across the size of the beamspot on the sample with respect to the penetration depth of the incident and fluorescence photons (for oxygen EXAFS ≈ 2000 Å). In the case where the contrary is true, different local geometries with different geometrical factors g occur and the dependence of the self-absorption

on the detection geometry becomes less pronounced. For (well-polished) single crystals or thin films deposited on a substrate material this condition holds true whereas for typical powder samples it may generally not be fulfilled.

(4) The fluorescence detector covers only a small solid angle around the sample, i.e., $\sqrt{A} \ll r$ with A being the sensitive area of the detector and r its distance from the sample. In this case, the angle θ and the geometrical factor g are well defined. However, for our experimental setup with $\theta = 90° - \phi$ even an acceptance angle of the fluorescence detector which corresponds to $\Delta\theta = 10°$ would alter the experimental spectra the most about 3%. The reason for this is that at grazing incidence angles ϕ the geometrical factor g is very insensitive to a variation of θ whereas at normal incidence angles even a larger variation of g does not have large effects on the spectra because the self-absorption itself is small.

Under the above conditions (1)–(4) the correction procedure for the self-absorption illustrated for the prototype NiO system is also applicable in general. It should apply at higher x-ray energies as well. However, using large area ionization chambers for the FY detection or powder samples, the latter two conditions may not be fulfilled. In a recent study of the high-T_c superconductor $YBa_2Cu_3O_7$ (Ref. 12) it was already shown that a correction of the self-absorption effect is necessary for a quantitative understanding of the oxygen FLEXAFS spectra. The full correction of the self-absorption effect given here, yielding the true EXAFS, allows in the cases of angular-dependent FLEXAFS measurements a detailed comparison and a quantitative analysis of the spectra.

V. INFORMATION DEPTH

We define the information depth λ_f of the FY detection as the expectation value of the depth perpendicular to the sample surface in which the detected fluorescence photons are generated. Under the assumptions made in Sec. III, the probability to detect a fluorescence photon generated in depth x in the sample is lower by the factor

$$\exp\left[-\left[\frac{\mu_{\rm tot}(E)}{\sin\phi}+\frac{\mu_{\rm tot}(E_f)}{\sin\theta}\right]x\right]$$

than the probability to detect one which is generated at the very surface. We therefore get

$$\lambda_f = \frac{\int_0^\infty x\exp\left[-\left[\frac{\mu_{\rm tot}(E)}{\sin\phi}+\frac{\mu_{\rm tot}(E_f)}{\sin\theta}\right]x\right]dx}{\int_0^\infty \exp\left[-\left[\frac{\mu_{\rm tot}(E)}{\sin\phi}+\frac{\mu_{\rm tot}(E_f)}{\sin\theta}\right]x\right]dx} = \frac{\sin\phi}{\mu_{\rm tot}(E)+\mu_{\rm tot}(E_f)g} \quad (8)$$

68% of the detected fluorescence photons are generated in a depth smaller than λ_f.

Figure 5 shows the information depth λ_f of the oxygen FLEXAFS of NiO calculated from Eq. (8) as a function of photoelectron wave vector for the detection geometries $\phi = 10°$, 25°, 40°, 55°, 70°, 85°, 88° (with $\theta = 90° - \phi$, see Fig. 1). At grazing x-ray incidence ($\phi = 10°$) as well as at normal x-ray incidence ($\phi = 85°$) the information depth is much smaller than for a detection geometry around $\phi = 45°$ where the incident and the detected fluorescence photons make equal angles with respect to the sample surface. This is also seen in the inset of Fig. 5 where the information depth at a photoelectron wave vector of $k = 6$, corresponding to the photon energy 670 eV, is shown as a function of x-ray incidence angle. For $\phi = 10°$ and $\phi = 85°$, the FY information depth is limited by the penetration depth of the incident and the detected fluorescence photons within the sample, respectively. This explains the energy independence of λ_f in the case of $\phi \geq 85°$ and its strong increase with photon energy for $\phi = 10°$. Figure 5 shows that in the soft x-ray region the information depth for a detection geometry with negligible self-absorption ($88° \lesssim \phi < 90°$, see Fig. 4) is $\lesssim 100$ Å, more than an order of magnitude lower than the maximal information depth which can be achieved. This is almost comparable to the information depth for TEY measurements $\lambda_e = 65$ Å, as determined by Jones *et al.*[20] at the aluminum K edge ($E = 1560$ eV). The TEY information depth at the oxygen K edge may be somewhat smaller.

Choosing a detection geometry with negligible self-absorption therefore makes the fluorescence detection very surface sensitive. To maintain the bulk sensitivity of FLEXAFS in the soft x-ray regime it may be necessary to measure under a geometry with considerable self-absorption and to be able to correct for it. Of course, in the case of a noncubic single crystalline material where

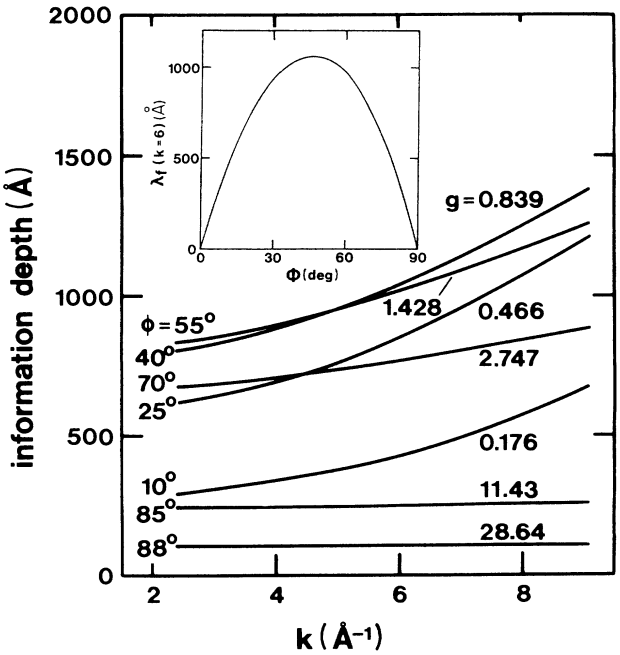

FIG. 5. The information depth λ_f of the FLEXAFS measurements in NiO as a function of photoelectron wave vector for different detection geometries. The inset shows the information depth at $k = 6$, corresponding to a fixed photon energy of 670 eV, as a function of x-ray incidence angle ϕ. It is seen that around $\phi = 45°$ FLEXAFS is the most bulk sensitive. Again $E_0 = 533$ eV was used for the conversion to k values.

the EXAFS of an unknown local environment is to be determined along different crystal orientations the freedom in choosing the detection geometry is limited unless samples with different crystal orientations can be manufactured. As another interesting application, the strong variation of the information depth of the FY detection with the detection geometry over about an order of magnitude could be used for depth-dependent measurements of the atomic local environment as, for example, in layered structures.

VI. CONCLUSION

We studied systematically distortions in the oxygen EXAFS of a NiO single crystal measured in fluorescence yield through the self-absorption effect by varying the experimental detection geometry. We showed that knowing the stoichiometry of the sample we can, based on an expression given already by Goulon *et al.*,[14] fully correct for the self-absorption and obtain the true, geometry-independent oxygen EXAFS of NiO from every single measured experimental spectrum. The correction assumes a thick sample, a plane sample surface and a detector covering a small solid angle but is otherwise generally applicable. Calculations starting from Eq. (1) or assuming a nonplane sample surface would give the correction in more complicated cases.

Because the proposed correction is made directly in k space previous to all data-analysis procedures, it is simple and can be easily included in the conventional EXAFS analysis. For certain applications, it should hold for FLEXAFS in the harder x rays as well. This correction is more general than earlier ones[9] in the sense that it (i) does not assume any particular energy dependence of the self-absorption effect and (ii) is not restricted to particular parameters related to the EXAFS amplitude. It should be the first step in the quantitative analysis of FLEXAFS measurements of concentrated samples. It may also allow to optimize the detection geometry for a maximal fluorescence information depth which in the soft x-ray region maintains the bulk sensitivity of FLEXAFS.

ACKNOWLEDGMENTS

We would like to thank H. Rabus (FU Berlin) for valuable and stimulating discussions as well as the BESSY staff for the help during the experiment. The work was partly supported by the BMFT (F&E Vorhaben 13N5740).

[1]J. Stöhr, in *X-Ray Absorption: Principles, Techniques and Applications of EXAFS, SEXAFS, and XANES,* edited by R. Prins and D. C. Koningsberger (Wiley, New York, 1985).

[2]J. Jaklevic, J. A. Kirby, M. P. Klein, A. S. Robertson, G. S. Brown, and P. Eisenberger, Solid State Commun. **23**, 679 (1977).

[3]F. Riehle, E. Tegeler, and B. Wende, Soft X-Ray Opt. Technol. **733**, 486 (1986).

[4]D. A. Fischer, U. Döbler, D. Arvanitis, L. Wenzel, K. Baberschke, and J. Stöhr, Surf. Sci. **177**, 114 (1986); D. Arvanitis, U. Döbler, L. Wenzel, K. Baberschke, and J. Stöhr, J. Phys. (Paris) Colloq. **47**, C8-173 (1986).

[5]M. Krumsey, E. Tegeler, and G. Ulm, Rev. Sci. Instrum. **60**, 2287 (1989).

[6]G. C. Smith, A. Krol, and Y. H. Kao, Nuclear Instrum. Methods Phys. Res. A **291**, 135 (1990).

[7]L. Tröger, D. Arvanitis, H. Rabus, L. Wenzel, and K. Baberschke, Phys. Rev. B **41**, 7297 (1990).

[8]See, for example, T. M. Hayes, and J. B. Boyce, in *Solid State Physics 37,* edited by H. Ehrenreich, F. Seitz, and D. Turnbull (Academic, New York, 1983), p. 256.

[9]Z. Tan, J. I. Budnick, and S. M. Heald, Rev. Sci. Instrum. **60**, 1021 (1989).

[10]Y. Suzuki, Phys. Rev. B **39**, 3393 (1989).

[11]D. M. Pease, D. L. Brewe, Z. Tan, J. I. Budnick, and C. C. Law, Phys. Lett. A **138**, 230 (1989).

[12]L. Tröger, D. Arvanitis, H. Rabus, K. Baberschke, and B. Stritzker, in *X-Ray Absorption Fine Structure,* edited by Samar Hasnain (Ellis Horwood, Chichester, England, 1991), p. 616.

[13]E. Zschech, L. Tröger, D. Arvanitis, H. Michaelis, U. Grimm, and K. Baberschke, Solid State Commun. **82**, 1 (1992).

[14]J. Goulon, C. Goulon-Ginet, R. Cortes, and J. M. Dubois, J. Phys. **43**, 539 (1982).

[15]H. Petersen, Nucl. Instrum. Methods **A246**, 260 (1986).

[16]L. Tröger, Diplom Thesis, Free University of Berlin, 1990 (unpublished).

[17]J. J. Yeh, and I. Lindau, At. Data Nucl. Data Tables **32**, 1 (1985).

[18]It is $\mu(\mathrm{cm}^{-1})=\mu(\mathrm{barns/atom})(1.66^{-1})M^{-1}(\mathrm{mol/g})\rho(g/\mathrm{cm}^3)$ with M and ρ being the atomic weight and the density of the element, respectively.

[19]*Handbook of Chemistry and Physics,* 67th edition, edited by R. C. Weast (CRC Press, Boca Raton, 1986), p. B110.

[20]R. G. Jones, and D. P. Woodruff, Surf. Sci. **114**, 38 (1982).